Entanglement in the above-threshold optical parametric oscillator

Alessandro S. Villar and Katiúscia N. Cassemiro

Instituto de Física, Universidade de São Paulo, Caixa Postal 66318, 05315-970 São Paulo, São Paulo, Brazil

Kaled Dechoum and Antonio Z. Khoury

Instituto de Física da Universidade Federal Fluminense, Boa Viagem, 24210-340, Niterói, Rio de Janeiro, Brazil

Marcelo Martinelli and Paulo Nussenzveig

Instituto de Física, Universidade de São Paulo, Caixa Postal 66318, 05315-970 São Paulo, São Paulo, Brazil

Received May 12, 2006; accepted June 27, 2006;
posted September 5, 2006 (Doc. ID 70938); published January 26, 2007

We investigate entanglement in the above-threshold optical parametric oscillator, both theoretically and experimentally, and discuss its potential applications to quantum information. The fluctuations measured in the subtraction of signal and idler amplitude quadratures are $\Delta^2\hat{p}_-=0.50(1)$, or $-3.01(9)$ dB, and in the sum of phase quadratures they are $\Delta^2\hat{q}_+=0.73(1)$, or $-1.37(6)$ dB. A detailed experimental study of the noise behavior as a function of pump power is presented, and the discrepancies with theory are discussed. © 2007 Optical Society of America

OCIS codes: 270.0270, 270.6570, 190.4970.

1. INTRODUCTION

The optical parametric oscillator (OPO) has been studied since the 1960s.[1,2] In the 1980s it was already recognized as an important tool in quantum optics for the generation of squeezed states of light.[3,4] It was also recognized as a suitable system for the demonstration of continuous variable (CV) entanglement in 1988 by Reid and Drummond[5] who considered the above-threshold operation. In the early 1990s, CV entanglement was indeed demonstrated for the first time in an OPO, although operating below threshold.[6] The OPO has since been used in several applications in CV quantum information.[7–11] Entanglement in the above-threshold OPO, on the other hand, remained an experimental challenge until 2005, when it was first observed by Villar *et al.*,[12] and subsequently by two other groups.[13,14]

Bipartite CV entanglement can be demonstrated by a violation of the following inequality, obtained independently by Duan *et al.*[15] and Simon:[16]

$$\Delta^2\hat{p}_- + \Delta^2\hat{q}_+ \geq 2, \tag{1}$$

where $\hat{p}_-=(\hat{p}_1-\hat{p}_2)/\sqrt{2}$ and $\hat{q}_+=(\hat{q}_1+\hat{q}_2)/\sqrt{2}$ are Einstein–Podolsky–Rosen (EPR) -type operators constructed by combining operators of each subsystem. We chose $\hat{p}_j$ and $\hat{q}_j$, $j\in\{0,1,2\}$, as the amplitude and phase quadrature operators of the pump, signal, and idler fields, respectively, which obey the commutation relations $[\hat{p}_j,\hat{q}_k]=2i\delta_{jk}$. Any separable system must satisfy Eq. (1); a violation is an unequivocal signature of entanglement.

Entanglement between the intense signal and idler beams generated by an above-threshold OPO can be physically understood as a consequence of energy conservation in the parametric process. On one hand, pump photons are converted into pairs of signal and idler photons, leading to strong intensity correlations; on the other hand, the sum of the frequencies of signal and idler photons is fixed to the value of pump frequency, leading to phase anticorrelations. The difficulty of measuring phase fluctuations was largely responsible for the long time between the prediction and the first observation of entanglement in the above-threshold OPO. The technique we used to measure phase fluctuations consists of reflecting each field off an empty optical cavity, as explained in Ref. 17.

The value of Eq. (1) obtained in the first demonstration of entanglement was 1.41(2), with squeezing observed in both EPR-type operators, $\Delta^2\hat{p}_-=0.59(1)$ and $\Delta^2\hat{q}_+=0.82(2)$.[12] Nevertheless, such a result could be achieved only very close to threshold, otherwise the phase sum $\Delta^2\hat{q}_+$ would present excess noise, increasing with pump power relative to the threshold $\sigma=P_0/P_{\mathrm{th}}$. This strange behavior, also observed by other groups,[18] is not predicted by the standard linearized OPO theory for a shot-noise limited pump beam. According to this model, entanglement should exist for all values of σ, although the degree of entanglement should decrease for increasing σ. This presented an additional complication for the first demonstration of entanglement in the above-threshold OPO.

In this paper we present new improved results of entanglement in the above-threshold OPO, together with a theoretical and experimental study of this unexpected excess phase sum noise. The paper is organized as follows. We begin by describing the linearized model for the OPO and its predictions for a shot-noise limited pump beam.

 © 2007 Optical Society of America

This model includes losses and also allows for nonvanishing detunings of pump, signal, and idler modes with respect to the OPO cavity. We then present a full-quantum treatment, neglecting losses and for zero detunings. Even after eliminating the linearization approximation, the theory does not predict the observed excess noise. The experiment is described next, and we present the measurements of the sum and difference of the quadrature fluctuations as a function of σ. As we will see, the excess noise in the phase sum can be related to pump noise generated inside the OPO cavity. Finally we present our current best measurement of two-color squeezed-state entanglement. We conclude by mentioning applications of this entanglement in quantum information.

2. THEORETICAL DESCRIPTION OF THE OPTICAL PARAMETRIC OSCILLATOR

The OPO consists of three modes of the electromagnetic field coupled by a nonlinear crystal, which is held inside an optical cavity. The OPO is driven by an incident pump field at frequency ω_0. Following the usual terminology, the downconverted fields are called the signal and the idler of frequencies ω_1 and ω_2, where, by energy conservation $\omega_0 = \omega_1 + \omega_2$. Here we will treat the case of a cavity that is triply resonant for ω_0, ω_1, and ω_2. Each field is damped via the cavity output mirror, thereby interacting with reservoir fields. The effective second-order nonlinearity of the crystal is represented by the constant χ.

Reid and Drummond investigated the correlations in the nondegenerate OPO (NOPO) both above[19] and below threshold.[20] In the above-threshold case, they studied the effects of phase diffusion in the signal and idler modes, beginning with the positive P-representation equations of motion for the interacting fields.[21,22] Changing to intensity and phase variables, they were able to show that output quadratures could be chosen that exhibited fluctuations below the coherent state level and also EPR-type correlations. In the below-threshold case, a standard linearized calculation was sufficient to obtain similar correlations. In the limit of a rapidly decaying pump mode, Kheruntsyan and Petrosyan were able to calculate the exact steady-state Wigner function for the NOPO, showing clearly the threshold behavior and the phase diffusion above this level of pumping.[23] We begin by describing the linearized model, and then proceed to calculate the noise spectra beyond linearization.

A. Linearized Model

The equations describing the evolution of signal, idler, and pump amplitudes, α_j, inside the triply resonant OPO cavity are given below.[17] They are obtained by writing the density operator equation of motion in the Wigner representation, and then searching for a set of equivalent Langevin equations,

$$\tau\frac{\mathrm{d}}{\mathrm{d}t}\alpha_0 = -\gamma_0'(1-i\Delta_0)\alpha_0 - 2\chi^*\alpha_1\alpha_2 + \sqrt{2\gamma_0}\alpha_0^{\mathrm{in}} + \sqrt{2\mu_0}\delta v_0,$$

$$\tau\frac{\mathrm{d}}{\mathrm{d}t}\alpha_1 = -\gamma'(1-i\Delta)\alpha_1 + 2\chi\alpha_0\alpha_2^* + \sqrt{2\gamma}\delta u_1 + \sqrt{2\mu}\delta v_1,$$

$$\tau\frac{\mathrm{d}}{\mathrm{d}t}\alpha_2 = -\gamma'(1-i\Delta)\alpha_2 + 2\chi\alpha_0\alpha_1^* + \sqrt{2\gamma}\delta u_2 + \sqrt{2\mu}\delta v_2, \tag{2}$$

where γ and γ_0 are half the transmissions of the mirrors, γ' and γ_0' are the total intracavity losses, $\mu = \gamma' - \gamma$ and $\mu_0 = \gamma_0' - \gamma_0$ are the spurious intracavity losses, Δ and Δ_0 are the detunings of the OPO cavity relative to the central frequencies of the fields, and τ is the cavity roundtrip time. We have considered here that $\gamma_1 = \gamma_2 = \gamma$ and $\gamma_1' = \gamma_2' = \gamma'$. The parameter χ is the effective second-order nonlinearity. The terms δu_j and δv_j are vacuum fluctuations associated to the losses from transmissions from the mirrors and from spurious sources, respectively. In the case of the intracavity pump mode, the fluctuations that come from the mirror transmission are attributable to the quantum fluctuations of the input pump laser beam, $\delta\alpha_0^{\mathrm{in}} = \delta p_0^{\mathrm{in}} + i\,\delta q_0^{\mathrm{in}}$.

Linearization consists in writing $\alpha_j(t) = e^{i\phi_j}(p_j + \delta p_j(t) + i\,\delta q_j(t))$ and ignoring terms that involve products of fluctuations in the equations. Here $\langle\alpha_j\rangle = p_j e^{i\phi_j}$ is each field's mean amplitude, with $p_1 = p_2 \equiv p$ for equal overall intracavity losses in the signal and the idler, $\delta p_j(t)$ is the amplitude fluctuation, and $\delta q_j(t)$ is the phase fluctuation. Taking the average of the resulting equations gives us information on the mean values of the fields. We may then separate the fluctuating part in the real and imaginary contributions to obtain the equations of evolution for the quadratures of the fields. Defining $\delta q_\pm = (\delta q_1 \pm \delta q_2)/\sqrt{2}$ and $\delta p_\pm = (\delta p_1 \pm \delta p_2)/\sqrt{2}$ as the normalized sum–subtraction of the signal and the idler amplitude and phase quadratures, we write the above equations in terms of the EPR variables:

$$\tau\frac{\mathrm{d}}{\mathrm{d}t}\delta p_- = -2\gamma'\,\delta p_- + \sqrt{2\gamma}\delta u_{p_-} + \sqrt{2\mu}\delta v_{p_-},$$

$$\tau\frac{\mathrm{d}}{\mathrm{d}t}\delta q_- = 2\Delta\gamma'\,\delta p_- + \sqrt{2\gamma}\delta u_{q_-} + \sqrt{2\mu}\delta v_{q_-},$$

$$\tau\frac{\mathrm{d}}{\mathrm{d}t}\delta p_+ = -2\Delta\gamma'\,\delta q_+ + \sqrt{2}\gamma'\beta\delta p_0 + \sqrt{2}\Delta\gamma'\beta\delta q_0 + \sqrt{2\gamma}\delta u_{p_+} + \sqrt{2\mu}\delta v_{p_+},$$

$$\tau\frac{\mathrm{d}}{\mathrm{d}t}\delta q_+ = -2\gamma'\,\delta q_+ - \sqrt{2}\Delta\gamma'\beta\delta p_0 + \sqrt{2}\gamma'\beta\delta q_0 + \sqrt{2\gamma}\delta u_{q_+} + \sqrt{2\mu}\delta v_{q_+},$$

$$\tau\frac{\mathrm{d}}{\mathrm{d}t}\delta p_0 = -\sqrt{2}\gamma'\beta\delta p_+ + \sqrt{2}\Delta\gamma'\beta\delta q_+ - \gamma_0'\delta p_0 - \Delta_0\gamma_0'\delta q_0 + \sqrt{2\gamma_0}\delta p_0^{in} + \sqrt{2\mu_0}\delta v_{p_0},$$

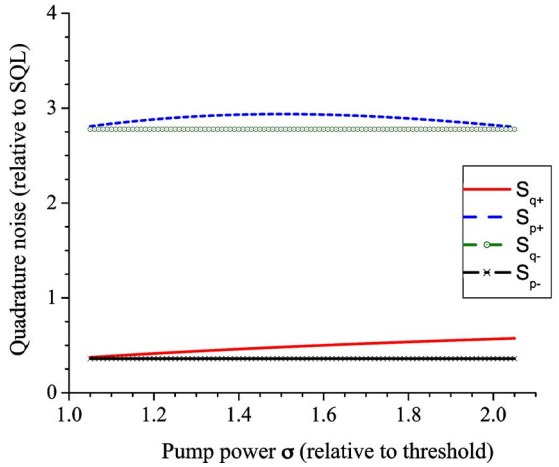

Fig. 1. (Color online) Prediction of the linearized theory for fluctuation in the sum–subtraction of field quadratures as a function of σ for a shot-noise limited pump beam. Solid line, S_{q_+}; dashed curve, S_{p_+}; line with crosses, S_{p_-}; line with circles, S_{q_-}.

$$\tau\frac{\mathrm{d}}{\mathrm{d}t}\delta q_0 = -\sqrt{2}\Delta\gamma'\beta\delta p_+ - \sqrt{2}\gamma'\beta\delta q_+ + \Delta_0\gamma_0'\delta p_0 - \gamma_0'\delta q_0 + \sqrt{2\gamma_0}\delta q_0^{in} + \sqrt{2\mu_0}\delta v_{q_0}, \tag{3}$$

where $\beta = p/p_0$ is the ratio between the intracavity amplitudes of the downconverted and the pump fields. The noise spectra of the transmitted fields are calculated by solving the above equations in Fourier space. We define $S_{p\pm}$ and $S_{q\pm}$ as the noise spectra of the operators $\hat{p}_\pm$ and $\hat{q}_\pm$, respectively.

It is clear from Eq. (3) that the quadrature subtraction subspace decouples from the others, so that S_{q_-} and S_{p_-} depend only on the ratio of losses through the output cavity mirror to the total intracavity losses and on the analysis frequency Ω. These fluctuations do not depend on pump power, and are in a minimum uncertainty state, $S_{p_-}\times S_{q_-} = 1$, if $\gamma = \gamma'$.

On the other hand, the sum of the quadratures and pump field subspaces are connected. This directly implies that excess noise in the pump beam degrades signal–idler entanglement, and can even destroy it.[17] The behavior of the twin beams' fluctuations as functions of pump power relative to threshold σ, for a shot-noise limited pump, is presented in Fig. 1. The maximum squeezing of S_{q+} occurs at threshold, and approaches shot noise for higher pump powers.

This behavior changes in the presence of excess noise in the pump. In that case, both S_{q+} and S_{p+} increase from their values at threshold. In particular, S_{q+} goes from squeezing to excess noise. The point where it crosses the shot noise value depends solely on the amount of excess phase noise present in the pump beam. For this reason, it was necessary to filter the pump field in the experiment, in order to observe entanglement.

B. Noise Spectra beyond the Linearized Model

We present here a comparison between the linearized approach to the quantum noise in the OPO and the numerical integration of the quantum stochastic equations in the positive P representation. This will help us to eliminate the linearization procedure as the reason for the discrepancy between the theoretical prediction of squeezing and the experimentally observed excess phase noise for $\sigma > 1.2$. We shall follow the procedure used in Ref. 24.

Although exact Heisenberg equations of motion can be found for this system, it is, at the very least, extremely difficult to solve nonlinear operator equations. Therefore we develop stochastic equations of motion in the positive P representation, which in principle give access to any normally ordered operator expectation values we may wish to calculate. To find the appropriate equations, we proceed via the master and Fokker–Planck equations. Using the standard techniques for elimination of the baths,[25] we find the zero-temperature master equation for the reduced density operator. The master equation may be mapped onto a Fokker–Planck equation[26] for the positive-P pseudoprobability distribution.

The cavity damping rates at each frequency are $\gamma^D = 2\gamma/\tau$, with $\gamma_1 = \gamma_2 = \gamma$. We further define $\gamma_r = \gamma_0/\gamma$. To apply the perturbation theory, we introduce a normalized coupling constant

$$g = \frac{\chi}{\gamma^D\sqrt{2\gamma_r}}, \tag{4}$$

which will be a power expansion parameter. Moreover, it will be useful to work with the scaled quadratures

$$\begin{aligned} x_0 &= g\sqrt{2\gamma_r}p_0, & q_0 &= g\sqrt{2\gamma_r}q_0, \\ x_+ &= gp_+, & y_+ &= gq_+, \\ x_- &= gp_-, & y_- &= gq_-, \end{aligned} \tag{5}$$

to render the stochastic equations amenable to perturbation. The stochastic equations for the scaled EPR variables become

$$\begin{aligned} \frac{\mathrm{d}x_0}{\mathrm{d}T} &= -\gamma_r\left[x_0 - 2\sqrt{\sigma} + \frac{1}{2}(x_+^2 - x_-^2 - y_+^2 + y_-^2)\right], \\ \frac{\mathrm{d}y_0}{\mathrm{d}T} &= -\gamma_r[y_0 + x_+y_+ - x_-y_-], \\ \frac{\mathrm{d}x_-}{\mathrm{d}T} &= -x_- - \frac{1}{2}[x_0x_- + y_0y_-] + \frac{g}{\sqrt{2}}[\sqrt{x_0 + iy_0}\xi_- + \sqrt{x_0 - iy_0}\xi_-^+], \\ \frac{\mathrm{d}y_+}{\mathrm{d}T} &= -y_+ + \frac{1}{2}[y_0x_+ - x_0y_+] - i\frac{g}{\sqrt{2}}[\sqrt{x_0 + iy_0}\xi_+ - \sqrt{x_0 - iy_0}\xi_+^+], \\ \frac{\mathrm{d}x_+}{\mathrm{d}T} &= -x_+ + \frac{1}{2}[x_0x_+ + y_0y_+] + \frac{g}{\sqrt{2}}[\sqrt{x_0 + iy_0}\xi_+ + \sqrt{x_0 - iy_0}\xi_+^+], \\ \frac{\mathrm{d}y_-}{\mathrm{d}T} &= -y_- + \frac{1}{2}[x_0y_- - y_0x_-] - i\frac{g}{\sqrt{2}}[\sqrt{x_0 + iy_0}\xi_- - \sqrt{x_0 - iy_0}\xi_-^+], \end{aligned} \tag{6}$$

where $T = \gamma^D t$ is time in units of the cavity lifetime for the downconverted fields. The functions $\xi_\pm(T)$ and $\xi_\pm^+(T)$ are independent Langevin forces with the following nonvanishing correlation functions:

$$\langle \xi_+(T)\xi_+(T')\rangle = \langle \xi_+^+(T)\xi_+^+(T')\rangle = \delta(T-T'),$$

$$\langle \xi_-(T)\xi_-(T')\rangle = \langle \xi_-^+(T)\xi_-^+(T'T)\rangle = -\delta(T-T'). \quad (7)$$

We notice the symmetry properties of the stochastic Eqs. (6). In fact, it is easy to verify that the equations of motion are unchanged by the transformation $x_- \leftrightarrow y_+$ and $x_+ \leftrightarrow -y_-$. Of course, all noise terms appearing in Eqs. (6) are statistically equivalent. Therefore these equations should not change the symmetries of the initial values chosen for x_+ and y_-.

To provide a comparison between the linearized model and the full stochastic integration, we will use a perturbation expansion of the positive P representation of the dynamical equations. This allows us to include quantum effects in a systematic fashion.[27] We first introduce a formal perturbation expansion in powers of the parameter g:

$$x_k = \sum_{n=0}^{\infty} g^n x_k^{(n)},$$

$$y_k = \sum_{n=0}^{\infty} g^n y_k^{(n)}. \quad (8)$$

The series expansion written in this way has the property that the zeroth-order term corresponds to the classical field of order 1 in the unscaled quadrature, while the first-order term is related to quantum fluctuations of order g, and the higher-order terms correspond to the nonlinear corrections to the quantum fluctuations of order g^2 and greater. The stochastic equations are then solved by the technique of matching powers of g in the corresponding time evolution equations.

The steady-state solutions x_{js} of the zeroth order give the operation point of the OPO and describe its macroscopic behavior. For a triply resonant operation, the expressions for the steady state are quite simple:

$$x_{0s} = 2,$$

$$x_{+s} = 2(\sqrt{\sigma}-1)^{1/2},$$

$$x_{-s} = 0,$$

$$y_{0s} = y_{+s} = y_{-s} = 0. \quad (9)$$

The first-order equations are often used to predict squeezing in a linearized fluctuation analysis. They are nonclassical in the sense that they can describe states without a positive-definite Glauber–Sudarshan P distribution,[28,29] but correspond to a simple form of linear fluctuation that has a Gaussian quasi-probability distribution. A full quantum description of the OPO dynamics can be obtained by a numerical integration of the stochastic Eqs. (6), and can be compared to analytical expressions obtained from the linearized approach. Taking the first-order terms and using the steady-state solutions given by Eqs. (9), we can write the following equations for the linear quantum fluctuations:

$$\frac{dx_0^{(1)}}{dT} = -\gamma_r[x_0^{(1)} + 2(\sqrt{\sigma}-1)^{1/2}x_+^{(1)}],$$

$$\frac{dy_0^{(1)}}{dT} = -\gamma_r[y_0^{(1)} + 2(\sqrt{\sigma}-1)^{1/2}y_+^{(1)}],$$

$$\frac{dx_+^{(1)}}{dT} = -(\sqrt{\sigma}-1)^{1/2}x_0^{(1)} + (\xi_+ + \xi_+^+),$$

$$\frac{dx_-^{(1)}}{dT} = -2x_-^{(1)} + (\xi_- + \xi^+),$$

$$\frac{dy_+^{(1)}}{dT} = -2y_+^{(1)} + (\sqrt{\sigma}-1)^{1/2}y_0^{(1)} - i(\xi_+ - \xi_+^+),$$

$$\frac{dy_-^{(1)}}{dT} = -i(\xi_- - \xi_-^+). \quad (10)$$

The linear coupled stochastic equations obtained agree with Eqs. (3), for zero detunings and no spurious losses. From them we may readily calculate the steady-state averages of the first-order corrections and use them to compute the linearized fluctuations. Notice that under the linear approximation y_- becomes a purely diffusive variable (phase diffusion).

In an experimental situation, the noise spectra outside the cavity are generally the quantities of interest. Therefore we will proceed to analyze the problem in frequency space, via a Fourier decomposition of the fields. The first-order stochastic equations may be rewritten in the frequency domain so that we may calculate the spectra of the squeezed and antisqueezed field quadratures.

The solutions for the noise of the squeezed operators, $\hat{p}_-$ and $\hat{q}_+$, are

$$S_{p_-}(\Omega') = 1 - \frac{1}{\Omega'^2+1}, \quad (11)$$

$$S_{q+}(\Omega') = 1 - \frac{(4\Omega'^2+\gamma_r^2)^2}{\Omega'^2[4\Omega'^2+\gamma_r^2-2\gamma_r(\sqrt{\sigma}-1)]^2+[4\Omega'^2+\gamma_r^2\sqrt{\sigma}]^2}, \quad (12)$$

where $\Omega' = \Omega/\gamma^D$ is the analysis frequency in units of the cavity bandwidth.

Under the limits of the linearized approach, the results of the noise spectra are independent of the phase space representation employed. Therefore these results coincide with the usual ones obtained with the Wigner representation.

The spectra given by Eqs. (11) and (12) can now be compared with those found via a stochastic integration of the full equations of motion (6) in the positive P representation. The nonlinear spectra are calculated by Fourier transform of the stochastic integration, which must be performed numerically. A somewhat subtle point arises

here: the nonlinear Eqs. (6) have more than one possible steady-state solution. Thus for a fair comparison with the linearized spectra, it is necessary to choose the same steady state. By doing this, we verified that both predictions, in the above-threshold OPO, agree within a good numerical precision. Therefore we conclude that possible limitations of the linearized model for dealing with the OPO dynamics under phase diffusion do not account for the experimentally observed excess noise of $\hat{q}_+$.

3. EXPERIMENT

Our system is a triply resonant type-II OPO operating above threshold. The experimental setup is depicted in Fig. 2. The pump beam is a diode-pumped doubled Nd:YAG laser (Innolight Diabolo) with 900 mW output power at 532 nm. A secondary output at 1064 nm is used for alignment purposes. Since the pump beam presents excess noise for frequencies as high as 20 MHz, a filter cavity is necessary. Our filter cavity has a bandwidth of 2.4 MHz and assures that the pump laser is shot-noise limited for analysis frequencies higher than 15 MHz (see Fig. 3). We measured the laser phase noise by reflecting the beam off an empty cavity, in the same way we measure the phase noise of the downconverted beams. The phase noise equals the intensity noise, except at a frequency of 12 MHz, where there is very big phase noise, owing to a frequency modulation inside the Diabolo laser for stabilization purposes. This excess noise saturates our electronics and prevents measurements for analysis frequencies close to 12 MHz and also to its second harmonic, 24 MHz, as can be seen in Fig. 3. The OPO cavity is a linear semimonolithic cavity composed of a flat input mirror, directly deposited on one face of the nonlinear crystal, with 93% reflectivity at 532 nm and high reflectivity (>99.8%) at 1064 nm, and a spherical output mirror (50 mm curvature radius) with high reflectivity at 532 nm (>99.8%) and 96% reflectivity at 1064 nm. The nonlinear crystal is a 10 mm long potassium titanyl phosphate (KTP) from Litton. The threshold power is 12 mW.

The signal and the idler beams are separated by a polarizing beam splitter (PBS) and sent to detection, which consists of a ring cavity and a photodetector (Epitaxx ETX 300) for each beam. The overall detection efficiency is $\eta = 80(2)\%$. Both analysis cavities have bandwidths of 14 MHz, allowing for a complete conversion of phase to amplitude noise for analysis frequencies higher than 20 MHz. The measurements are taken at an analysis frequency equal to 27 MHz. To access the same quadrature

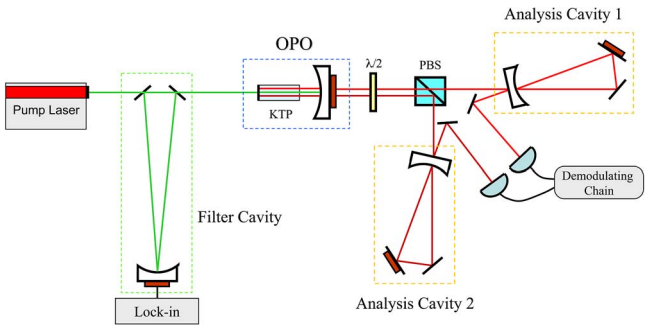

Fig. 2. (Color online) Sketch of the experimental setup.

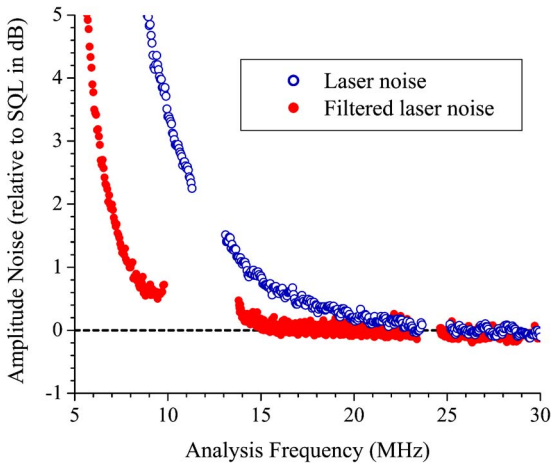

Fig. 3. (Color online) Measurement of the pump noise as a function of the analysis frequency. Open circles, unfiltered laser noise; full circles, laser noise at the output of the filter cavity. In view of the large excess noise at 12 MHz and its second harmonic, we suppressed those frequencies from the data.

for both beams, the two cavities must be detuned by the same amount at the same time. By scanning the detunings synchronously, we can measure all quadratures of the twin beams. In particular, we can easily select the amplitude (off resonance) or phase (detuning equal to one-half the bandwidth) quadratures.[30]

The data acquisition is carried out by a demodulating chain, which mixes the photocurrents from each detector with a sinusoidal electronic reference at the analysis frequency and filters the resulting low-frequency signal. The demodulated photocurrent fluctuations are sampled at 600 kHz repetition rate by an analog-to-digital (A/D) card connected to a personal computer. The variances of these fluctuations are then computed taking groups of 1000 points, resulting in something proportional to the power spectrum of the photocurrents at the analysis frequency. At the end, measured variances are normalized to the shot noise standard quantum level (SQL).

A. Fluctuations as a Function of σ

The input pump field is guaranteed to be shot-noise limited for frequencies above 15 MHz after being transmitted through the filter cavity. Even before being filtered, the pump field is shot-noise limited above 25 MHz, as shown in Fig. 3. Nevertheless, we observed excess noise in the sum of the phases of the signal and the idler beams, preventing the violation of the inequality given in Eq. (1) except for pump powers very close to threshold.[12]

As seen in Section 2 from the theoretical description of the OPO, excess noise in the pump beam would generate excess noise in the phase sum of the twin beams. Yet how could that be the case if we carefully measured the input pump to be shot-noise limited? By following this single lead, it is natural to examine the noise properties of the pump beam reflected from the OPO cavity. This was done by scanning the OPO cavity for crystal temperatures such that there was no parametric oscillation (triple resonance depends sharply on crystal temperature and can easily be avoided). Since the incident beam is shot-noise limited, could there be excess noise generated inside the cavity

containing the KTP crystal? We did indeed find excess noise in the reflected pump's amplitude (Fig. 4) and phase quadratures. The maximum values, for $\sigma=1$, were $S_{p0}^{R}=1.8(1)$ and $S_{q0}^{R}=4.5(3)$.

At present, we can still not claim to fully understand the origin of this excess noise. We verified, of course, that no such noise is generated in an empty cavity (which would also invalidate the measurements we perform with the analysis cavities for the twin beams). We also checked whether this effect depended on χ and would thus be directly related to the parametric process. For a polarization of the incident beam orthogonal to the usual polarization, phase matching cannot be fulfilled, and no downconversion can occur. The noise in the reflected beam did not show any significant dependence on the incident polarization. It does, however, increase for increasing power of the incident beam. We can speculate that this can be a result of photon absorption by the crystal at 532 nm (which is at the origin of the thermal bistability observed in Fig. 4), with a subsequent relaxation by spontaneous emission or nonradiative processes. This, may give rise to an intensity-dependent refractive index, yielding phase and amplitude modulation at 532 nm. We are currently investigating these possibilities.

As a first approximation, in order to see whether this would account for the behavior of $\Delta^2\hat{p}_-,\Delta^2\hat{q}_-,\Delta^2\hat{p}_+$, and $\Delta^2\hat{q}_+$, as a function of σ, we simply added excess noise to the input pump beam in the linearized OPO theory. In Fig. 5 we compare the results from the model, with incident $S_{p0}=1.5$ and $S_{q0}=5.5$, to the measured data. The signal and idler powers varied from 0.4 up to 5.5 mW each during the experiment, corresponding to pump powers between 13 and 26 mW, or $1.06<\sigma<2.2$. As expected, noises corresponding to the subtraction subspace, $\Delta^2\hat{p}_-$ and $\Delta^2\hat{q}_-$, are independent of pump power. But $\Delta^2\hat{q}_+$ is very sensitive to σ, as is $\Delta^2\hat{p}_+$ to a lesser degree. The agreement with the theoretical model is surprisingly good. This is a strong indication that the intracavity pump excess noise is the main responsible for the excess noise in $\Delta^2\hat{q}_+$.

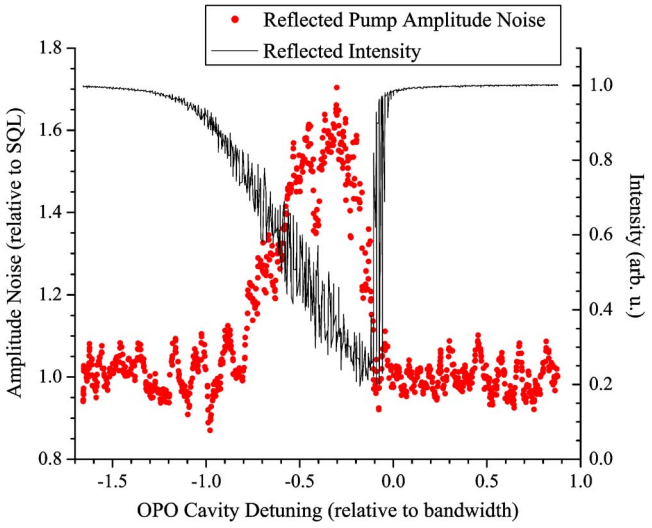

Fig. 4. (Color online) Intensity noise of the reflected pump beam, as a function of the detuning of the OPO cavity. The excess noise observed is peaked for Δ_0, close to one-half the OPO cavity bandwidth. The asymmetry in the mean-field signal is attributable to the thermal bistability. The analysis frequency is 27 MHz. Circles, reflected pump noise; full curve, reflected average intensity.

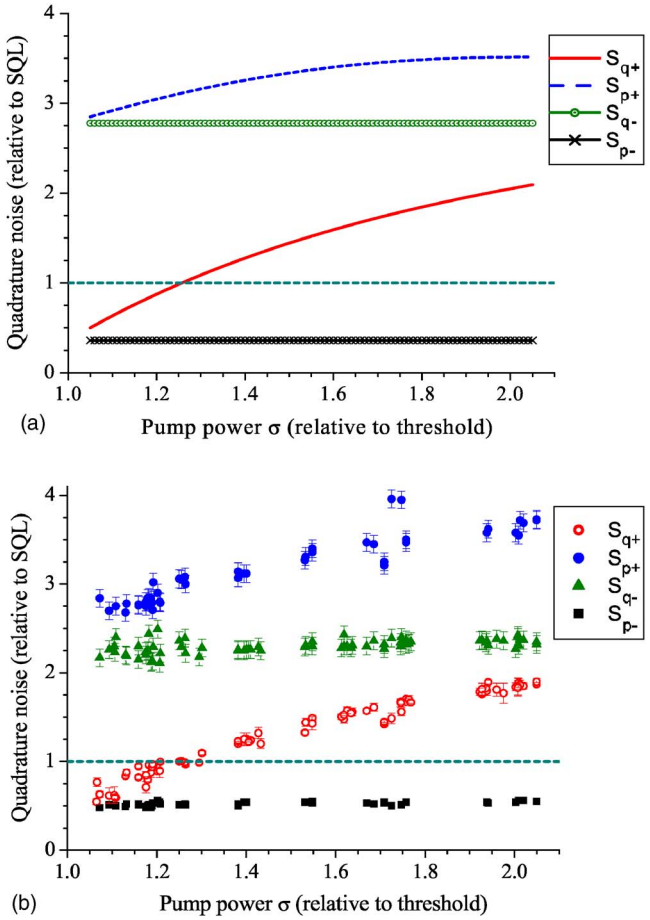

Fig. 5. (Color online) Noise behavior as a function of σ. (a) Predictions of the linearized model for an input pump beam with $S_{p_0}=1.5$ and $S_{q0}=5.5$; dashed curve, S_{p_+}; solid line with open circles, S_{q_-}, solid curve, S_{q_+}; solid line with crosses, S_{p_-}; SQL =1.0 is indicated by a dashed line. (b) Experimental result for σ ranging from 1.06 to 2.2. Full circles, S_{p_+}; triangles, S_{q_-}; open circles, S_{q_+}; squares, S_{p_-}; SQL=1.0 is indicated by a dashed line.

B. Two-Color Entanglement

The sum of the phase noise is squeezed very close to threshold, and the squeezing is degraded with increasing pump power. $\Delta^2\hat{q}_+$ crosses the shot-noise level approximately at $\sigma=1.20$, from squeezing to antisqueezing, although only below $\sigma=1.15$ can squeezing be observed with certainty.

Figure 6 shows the recorded noise in sum and subtraction of the photocurrent fluctuations of the signal and the idler beams as functions of the detuning of the analysis cavities for $\sigma=1.06$. Off-resonance, quantum correlations are observed in the subtraction of amplitudes, $\Delta^2\hat{p}_-=0.50(1)$, or $-3.01(9)$ dB. For detuning of analysis cavities equal to one-half the bandwidth, squeezing is present in the sum of phases, $\Delta^2\hat{q}_+=0.73(1)$, or $-1.37(6)$ dB. The Duan *et al.* and Simon criteria [Eq. (1)], are clearly violated:

$$\Delta^2\hat{p}_- + \Delta^2\hat{q}_+ = 1.23(2) < 2, \tag{13}$$

attesting to the entanglement. This value, together with the one reported by Jing *et al.*,[14] is the lowest achieved for

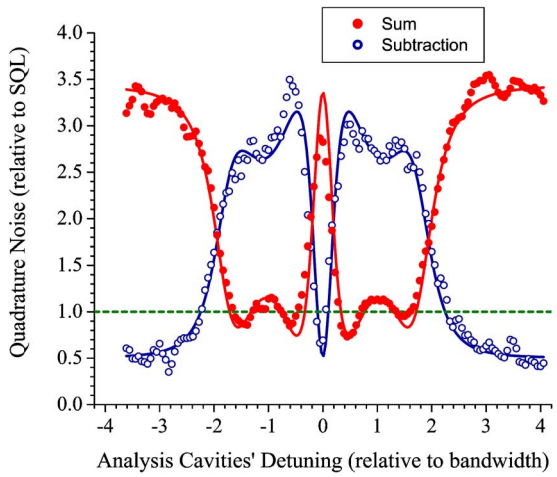

Fig. 6. Sum (full circles) and difference (open circles) of the quadrature noise measured as a function of the detuning of the analysis cavities. Squeezed-state entanglement can be directly observed, with $\Delta^2\hat{p}_-=0.50(1)$, or −3.01(9) dB, and $\Delta^2\hat{q}_+=0.73(1)$, or −1.37(6) dB.

twin beams produced by an above-threshold OPO.

We also point out that, in this experiment, the twin beams have very different frequencies (the wavelengths differ by ≈1 nm), an unusual situation. Such two-color entanglement can be very interesting for the transfer of quantum information between different parts of the electromagnetic spectrum.

4. CONCLUSION

We presented a theoretical and experimental investigation of phase noise and entanglement in the above-threshold OPO. Excess noise in the phase sum of the twin beams was measured as a function of pump power relative to threshold, and we found that it decreases as pump power is lowered. We finally discovered that excess pump noise is generated inside the OPO cavity containing the nonlinear crystal, even for a shot-noise limited pump beam and without parametric oscillation. The ultimate physical origin of this phenomenon still requires further investigation. Another important question to address is how one can eliminate this effect. Su *et al.*[13] were able to observe entanglement for σ of the order of 2. The difference between their setup and others is a lower cavity finesse for the pump field. If the assumption of an intensity-dependent index of refraction is correct, this makes sense. For a lower finesse, the phase shifts accumulated inside the cavity should be smaller, hence the excess noise generated should also be smaller.

In spite of these unexpected phenomena, two-color entanglement was measured in the above-threshold OPO. There are interesting avenues to pursue for applications in quantum information. First of all, we should mention that the strongest squeezing measured to date, −9.7 dB, was generated in an above-threshold OPO.[18] Thus, entanglement in the above-threshold OPO may be the strongest ever achieved for continuous variables. The bright twin beams can have very different frequencies, and one can envisage CV quantum teleportation[10] to transfer quantum information from one frequency to another (in other words, to tune quantum information). For example, this system could be used to communicate quantum information between quantum memories or quantum computers based on hardware that has different resonance frequencies. Finally, a quantum key distribution protocol proposed by Silberhorn *et al.*[31] can be readily implemented with the advantage that the measurement with analysis cavities does not require sending a local oscillator together with the quantum channel to the distant receiver.

The above-threshold OPO, which was the first system proposed to observe CV entanglement, has finally been added to the optical quantum information toolbox. We expect new and exciting applications to come in the near future.

ACKNOWLEDGMENTS

This work was supported by Fundação de Amparo à Pesquisa do Estado de São Paulo, Coordenação de Aperfeiçoamento de Pessoal de Nível Superior, and Conselho Nacional de Desenvolvimento Científico e Technológica through the Instituto do Milênio de Informação Quântica. We thank C. Fabre and T. Coudreau for lending us the nonlinear crystal.

The corresponding author P. Nussenzveig can be reached by e-mail at nussen@if.usp.br.

REFERENCES

1. R. H. Kingston, "Parametric amplification and oscillation of optical frequencies," Proc. IRE **50**, 472–474 (1962).
2. R. Graham and H. Haken, "The quantum fluctuations of the optical parametric oscillator," Z. Phys. **210**, 276–302 (1968).
3. L.-A. Wu, H. J. Kimble, J. L. Hall, and H. Wu, "Generation of squeezed states by parametric down conversion," Phys. Rev. Lett. **57**, 2520–2523 (1986).
4. A. Heidmann, R. J. Horowicz, S. Reynaud, E. Giacobino, C. Fabre, and G. Camy, "Observation of quantum noise reduction on twin laser beams," Phys. Rev. Lett. **59**, 2555–2557 (1987).
5. M. D. Reid and P. D. Drummond, "Quantum correlations of phase in nondegenerate parametric oscillation," Phys. Rev. Lett. **60**, 2731–2733 (1988).
6. Z. Y. Ou, S. F. Pereira, H. J. Kimble, and K. C. Peng, "Realization of the Einstein–Podolsky–Rosen paradox for continuous variables," Phys. Rev. Lett. **68**, 3663–3666 (1992).
7. S. L. Braunstein and P. van Loock, "Quantum information with continuous variables," Rev. Mod. Phys. **77**, 513–577 (2005).
8. W. P. Bowen, R. Schnabel, P. K. Lam, and T. C. Ralph, "Experimental investigation of criteria for continuous variable entanglement," Phys. Rev. Lett. **90**, 043601 (2003).
9. C. Schori, J. L. Sorensen, and E. S. Polzik, "Narrow-band frequency tunable light source of continuous quadrature entanglement," Phys. Rev. A **66**, 033802 (2002).
10. A. Furusawa, J. L. Sorensen, S. L. Braunstein, C. A. Fuchs, H. J. Kimble, and E. S. Polzik, "Unconditional quantum teleportation," Science **282**, 706–709 (1998).
11. X. J. Jia, X. L. Su, Q. Pan, J. G. Gao, C. D. Xie, and K. C. Peng, "Experimental demonstration of unconditional entanglement swapping for continuous variables," Phys. Rev. Lett. **93**, 250503 (2004).
12. A. S. Villar, L. S. Cruz, K. N. Cassemiro, M. Martinelli, and P. Nussenzveig, "Generation of bright two-color continuous variable entanglement," Phys. Rev. Lett. **95**, 243603 (2005).

13. X. L. Su, A. Tan, X. J. Jia, Q. Pan, C. D. Xie, and K. C. Peng, "Experimental demonstration of quantum entanglement between frequency-nondegenerate optical twin beams," Opt. Lett. **31**, 1133–1135 (2006).
14. J. Jing, S. Feng, R. Bloomer, and O. Pfister, "Experimental continuous-variable entanglement of phase-locked bright optical beams," arXiv.org archive, e-Print quant-ph/0604134 http://arxiv.org/abs/quantph/0604134.
15. L. M. Duan, G. Giedke, J. I. Cirac, and P. Zoller, "Inseparability criterion for continuous variable systems," Phys. Rev. Lett. **84**, 2722–2725 (2000).
16. R. Simon, "Peres–Horodecki separability criterion for continuous variable systems," Phys. Rev. Lett. **84**, 2726–2729 (2000).
17. A. S. Villar, M. Martinelli, and P. Nussenzveig, "Testing the entanglement of intense beams produced by a nondegenerate optical parametric oscillator," Opt. Commun. **242**, 551–563 (2004).
18. J. Laurat, L. Longchambon, C. Fabre, and T. Coudreau, "Experimental investigation of amplitude and phase quantum correlations in a type II optical parametric oscillator above threshold: from nondegenerate to degenerate operation," Opt. Lett. **30**, 1177–1179 (2005).
19. M. D. Reid and P. D. Drummond, "Correlations in nondegenerate parametric oscillation—squeezing in the presence of phase diffusion," Phys. Rev. A **40**, 4493–4506 (1989).
20. P. D. Drummond and M. D. Reid, "Correlations in nondegenerate parametric oscillation. 2. Below threshold results," Phys. Rev. A **41**, 3930–3949 (1990).
21. S. Chaturvedi, P. D. Drummond, and D. F. Walls, "2 photon absorption with coherent and partially coherent driving fields," J. Phys. A **10**, L187–L192 (1977).
22. P. D. Drummond and C. W. Gardiner, "Generalized *P*-representations in quantum optics," J. Phys. A **13**, 2353–2368 (1980).
23. K. V. Kheruntsyan and K. G. Petrosyan, "Exact steady-state Wigner function for a nondegenerate parametric oscillator," Phys. Rev. A **62**, 015801 (2000).
24. B. Coutinho dos Santos, K. Dechoum, A. Z. Khoury, L. F. da Silva, and M. K. Olsen, "Quantum analysis of the nondegenerate optical parametric oscillator with injected signal," Phys. Rev. A **72**, 033820 (2005).
25. H. J. Carmichael, *Statistical Methods in Quantum Optics 1: Master Equations and Fokker–Planck Equations* (Springer, 1999).
26. C. W. Gardiner, *Quantum Noise* (Springer-Verlag, 1991).
27. K. Dechoum, P. D. Drummond, S. Chaturvedi, and M. D. Reid, "Critical fluctuations and entanglement in the nondegenerate parametric oscillator," Phys. Rev. A **70**, 053807 (2004).
28. R. J. Glauber, "Coherent and incoherent states of the radiation field," Phys. Rev. **131**, 2766–2788 (1963).
29. E. C. G. Sudarshan, "Equivalence of semiclassical and quantum mechanical descriptions of statistical light beams," Phys. Rev. Lett. **10**, 277–279 (1963).
30. P. Galatola, L. A. Lugiato, M. G. Porreca, P. Tombesi, and G. Leuchs, "System control by variation of the squeezing phase," Opt. Commun. **85**, 95–103 (1991).
31. Ch. Silberhorn, N. Korolkova, and G. Leuchs, "Quantum key distribution with bright entangled beams," Phys. Rev. Lett. **88**, 167902 (2002).